Cu (In,Ga)Se_2 thin films and solar cells prepared by selenization of metallic precursors

Bülent M. Başol,[a] Vijay K. Kapur, Arvind Halani, and Craig R. Leidholm
International Solar Electric Technology, 8635 Aviation Boulevard, Inglewood, California 90301

Jon Sharp and James R. Sites
Physics Department, Colorado State University, Fort Collins, Colorado 80523

Amy Swartzlander, Richard Matson, and Harin Ullal
National Renewable Energy Laboratory (NREL), 1617 Cole Boulevard, Golden, Colorado 80401

(Received 20 November 1995; accepted 29 April 1996)

$CuIn_{(1-x)}Ga_xSe_2$ (CIGS) thin films with Ga ratio, x, ranging from 0.55 to 0.75 were grown on Mo/glass substrates by the selenization of metallic precursors in a H_2Se atmosphere. Without a postdeposition annealing step the films were found to have a highly graded composition that became Ga rich near the absorber/Mo interface. A high-temperature annealing step promoted diffusion of Ga to the surface region of the films. These absorbers were used to fabricate glass/Mo/CIGS/CdS/ZnO thin-film solar cells with open-circuit voltages ranging from 0.4 to 0.74 V and efficiencies approaching 12%. Devices, as well as the absorber layers, were characterized.

I. INTRODUCTION

$CuIn_{(1-x)}Ga_xSe_2$ (CIGS) chalcopyrite compound semiconductors of various compositions have received much attention as the absorber layers in high-efficiency polycrystalline thin-film solar cell structures. The energy band gap (E_g) of CIGS films can be varied continuously from about 1.0 to 1.7 eV by changing their composition from $CuInSe_2$ (CIS) to $CuGaSe_2$ (CGS). The variation of E_g with the Ga/(Ga+In) ratio is linear for Cu-poor material, whereas a definite bowing behavior in this relationship has been observed for stoichiometric films.[1] The possibility of band-gap control makes this quaternary semiconductor very attractive for high-efficiency thin-film solar cell structure designs employing graded band-gap absorber layers.

Among the various thin-film deposition techniques used for growing CIGS thin films, multisource evaporation and two-stage selenization are the two approaches that have yielded good quality absorbers. To date, the highest efficiency devices have been fabricated on CIGS films with graded Ga distribution obtained by a multisource evaporation technique.[2,3] Conversion efficiencies of solar cells fabricated by the methods of Ref. 2 have recently reached 17%.

Kushiya *et al.* prepared CIGS layers with uniform Ga and In distributions by the selenization of coevaporated Cu+In+Ga+Se precursor layers in a vacuum system and demonstrated a 14.9% efficient device on a film with a Ga/(Ga+In) ratio of 0.40.[4] The reported $E_g = 1.3$ eV for this absorber agreed with the expected value of 1.29 eV. Unlike the results of Kushiya *et al.* on films grown by the selenization of coevaporated Cu+In+Ga+Se precursor, coevaporated Cu+In+Ga metallic precursor layers always yielded absorbers with graded Ga concentrations when selenized in a vacuum system under Se vapor.[5] In such films, Ga-rich phase(s) segregated toward the back of the absorber layer, leaving an In-rich surface. Films grown by the selenization of Cu+In+Ga metallic precursors in H_2Se-containing atmospheres showed very similar behavior.[6,7] The reasons for this behavior are not well understood. However, it is possible that the In–Se reactions which are more energetically favorable at low temperatures form the driving force for In to selectively diffuse to the surface region to react with the selenizing atmosphere as the temperature of the substrate is raised.

Segregation of Ga-rich and In-rich phases by depth, in absorber layers obtained by the selenization of metallic precursors, does not allow the growth of CIGS films with uniform composition. A Ga-rich region deep in the absorber layer can benefit device performance because this high-band-gap area can induce an electric field in the bulk of the absorber and help minority carrier collection from deep in the device.[5] However, segregation of the Ga-rich and In-rich phases in a manner that leaves a small-band-gap CIS surface would limit the open-circuit voltage values of devices fabricated on such absorbers. In a recent publication, the research group of the Institute of Energy Conversion (IEC) at the University of Delaware demonstrated that films obtained by the selenization of metallic precursors displayed total segregation of CIS and CGS phases when further annealed in a H_2Se atmosphere at high temperatures. These researchers also described a new process consisting of a postselenization annealing step in a Se-free atmosphere, which was found to be essential to initiate the diffusion of Ga and formation of the quaternary CIGS phase.[6] It was concluded that the high-temperature annealing step in a Se-free atmosphere created Se vacancies through which Ga diffusion could be facilitated. Selenium vacancy generation resulting from high temperature annealing of CIS in a Se-free atmosphere is well established.[8] In this article, we employed the postselenization step of Ref. 6 to grow CIGS absorber layers with an overall Ga/(Ga+In) ratio of 0.55–0.75, characterized these layers in terms of their structural and compositional properties, and

[a]Electronic mail: bbasol@earthlink.net

evaluated their application to high-efficiency solar cell fabrication.

II. EXPERIMENTAL APPROACH

Soda-lime glass was used as the substrate in this work. Molybdenum layers of 2.0 μm thickness were sputter deposited on the soda-lime glass substrates using a dc magnetron system. CIGS absorber films were formed on the Mo/glass sheets by the two-stage selenization technique.[9] In this approach, a precursor layer containing In, Cu, and Ga was first deposited on the substrate by electron-beam evaporation. The precursor was then selenized in a 10% H_2Se+90% N_2 atmosphere to form the compounds. The precursor deposition step was carried out in one pump-down from a multipocket electron beam gun. A thin layer of Te (0.01 μm) was first evaporated on the Mo surface. Tellurium deposition was followed by the evaporation of In, Cu, and Ga in the given sequence. The evaporation rates were in the range of 10–50 Å/s. Inclusion of a thin Te layer in the precursor stack ensured proper wetting of the Mo surface by the evaporated In film and the formation of a uniform alloy precursor as discussed previously.[10] Thicknesses of the In, Cu, and Ga layers were adjusted to obtain films with various compositions and an overall stoichiometric ratio of about Cu/(In+Ga)=0.9. For the precursor of sample 1789-425 and 1789-575, the overall Ga/(Ga+In) ratio was 0.55 and the thicknesses of the evaporated In, Cu, and Ga layers as monitored by a crystal oscillator head were 2223, 2000, and 2027 Å, respectively. The Ga/(In+Ga) ratio for the precursor of samples 1791-425 and 1791-575, on the other hand, was 0.75, with corresponding elemental film thicknesses of 1228, 2000, and 2765 Å. The thicknesses quoted here were direct readings from the Inficon/XTC crystal oscillator. The stoichiometric ratios were calculated based on these actual readings.

Selenization was carried out for all precursors at 425 °C. A portion of each film was then additionally annealed at 575 °C in a N_2 atmosphere. Resulting selenide films were nominally 2.0 μm thick, and they were analyzed by scanning electron microscopy (SEM), x-ray diffraction (XRD), and Auger depth profiling. Auger analysis was carried out by a Physical Electronics 670 microprobe using a 5 kV electron beam. The samples were depth profiled using a 3 kV argon ion sputtering beam. A reference CIGS sample with uniform Ga distribution deposited at NREL by the coevaporation technique was used to calibrate the Auger sensitivity factors for Cu, In, Ga, and Se based on electron microprobe measurements. Devices were fabricated by depositing a thin layer of CdS on the CIGS layers by the solution growth technique. Conductive ZnO window layers were deposited by the metalorganic chemical vapor deposition (MOCVD) approach using diethylzinc (DEZ) and water vapor as the reactants and boron as the dopant. Details of the CdS and ZnO deposition steps have been published previously.[7] The resulting solar cell structure is shown in Fig. 1.

Devices were characterized by dark and illuminated current density–voltage (J–V), quantum efficiency (QE), and capacitance measurements. The charge collection efficiency profile was determined using cross-sectional electron-beam-induced-current (EBIC) techniques on cleaved cells.[11]

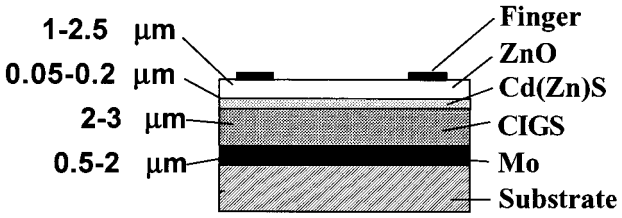

FIG. 1. Structure of a CIGS solar cell.

III. RESULTS AND DISCUSSION

A large number of absorber layers were grown and processed into solar cells during this study. The set of four absorbers that are the subject of this article is a typical subset of the larger lot of samples. Information about the overall stoichiometric compositions of the precursors and the processing steps employed to grow the selenide layers are given in Table I.

A. Device measurements

Figure 2 shows the illuminated J–V characteristics of solar cells fabricated on three of the absorber layers identified in Table I. The devices fabricated on sample 1791-425 were extremely leaky, and since they did not display a photovoltaic response, they were not included in Fig. 2.

The J–V characteristics of Fig. 2 indicate an open-circuit voltage (V_{oc}) value of 740 mV for sample 1791-575 and 625 mV for sample 1789-575. The V_{oc} for sample 1789-425, on the other hand, is only 400 mV despite the fact that this film contained 55% Ga. The absolute QE curves given in Fig. 3 were normalized using the short-circuit current values of the three devices. The losses due to various factors such as grid coverage and contact probe shadowing are shown in Fig. 3. Reflection, ZnO absorption, and CdS absorption measurements were made on a set of reference samples of CdS and ZnO on glass. The QE curves demonstrate that the effective band gaps of the three absorbers varied from 1.05 eV for sample 1789-425 to 1.36 eV for sample 1791-575. The solar cell output parameters derived from Fig. 2 as well as the E_g values are summarized in Table II. E_g values were deduced from the shift of the long wavelength QE of the cells

TABLE I. Information of the CIGS films grown for this study.

	Overall composition of the precursor		CIGS formation steps	
Sample No.	Cu/(In+Ga)	Ga/(Ga+In)	Selenization	Annealing
1789-425	0.9	0.55	425 °C, 30 min	
1789-575	0.9	0.55	425 °C, 30 min	575 °C, 60 min
1791-425	0.9	0.75	425 °C, 30 min	
1791-575	0.9	0.75	425 °C, 30 min	575 °C, 60 min

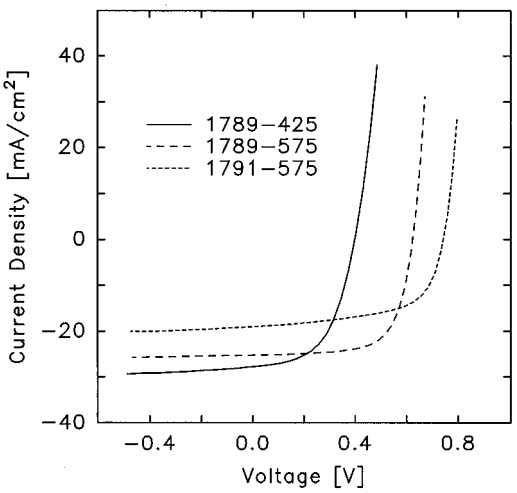

FIG. 2. Illuminated $J-V$ characteristics of three solar cells. Sample numbers are shown in the insert. Data were taken at 100 mW/cm^2 (AM1.5). The active area of the cells was 0.083 cm^2.

compared with a pure CIS device with the band-gap value of 1.00 eV. Long wavelength QE of the CIS cell is also shown in Fig. 3 for reference. The estimated uncertainty in the E_g values is 30 mV. The following observations can be made from the data of Table II.

(i) The band-gap value of sample 1789-425 deduced from its QE curve was much less than the 1.4 eV expected from a uniform CIGS layer with 55% Ga.[1] The observed value of $E_g = 1.05$ eV and correspondingly modest V_{oc} value of 400 mV, suggest the presence of a CIGS composition with only about 7% Ga in the absorber layer. Furthermore, the solar cell fabricated on this absorber is relatively poor with a low fill-factor value.

(ii) High-temperature annealing of sample 1789-425 increased the effective band gap of this absorber to 1.19 eV and V_{oc} to 625 mV, indicating increased Ga activity. However, this band gap is still lower than the 1.4 eV expected from a uniform CIGS layer with 55% Ga. The measured band-gap value of 1.19 eV indicates the presence of a CIGS phase in the absorber with about 28% Ga.

(iii) The QE data obtained from the cell fabricated on the annealed sample with an overall Ga content of 75% yielded a band-gap value of 1.36 eV and the device had a V_{oc} of 740 mV, which corresponds to a CIGS phase with about 50% Ga.

TABLE II. Solar cell parameters and band-gap values derived from the data of Figs. 2 and 3. The active area of the devices was 0.083 cm^2.

Sample No.	η (active area)	FF	V_{oc} (mV)	J_{sc} (mA/cm^2)	E_g (eV)
1789-425	6.4	0.54	400	30	1.05
1789-575	11.7	0.69	625	27.3	1.19
1791-575	9.4	0.615	740	20.6	1.36

The open-circuit voltages of the three devices of Fig. 2 were measured in the temperature range of 270–350 K. Extrapolation of V_{oc} to $T=0$ K gave an estimate of E_g, assuming it changes little over the temperature range used. The zero-temperature intercepts were 1.08, 1.25, and 1.34 eV for samples 1789-425, 1789-575, and 1791-575, respectively. These values are in reasonable agreement with the values obtained from QE data and are listed in Table II.

Figure 4 shows the cross-sectional EBIC line scans of two devices superimposed over their scanning electron images. The various layers forming the device structure are labeled in Fig. 4. The CIGS layers are dense and are composed of grains as large as 1–2 μm. The grain size does not seem to be a function of the high-temperature annealing step at

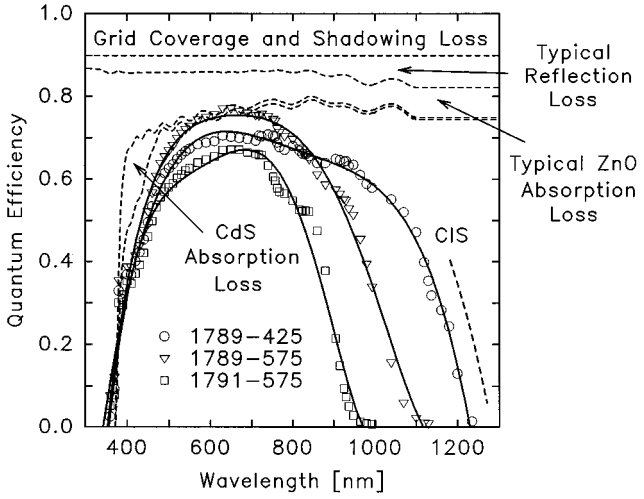

FIG. 3. Absolute quantum efficiencies of the cells of Fig. 2. The long wavelength portion of the QE data taken from a CIS cell (no Ga) is also shown for comparison.

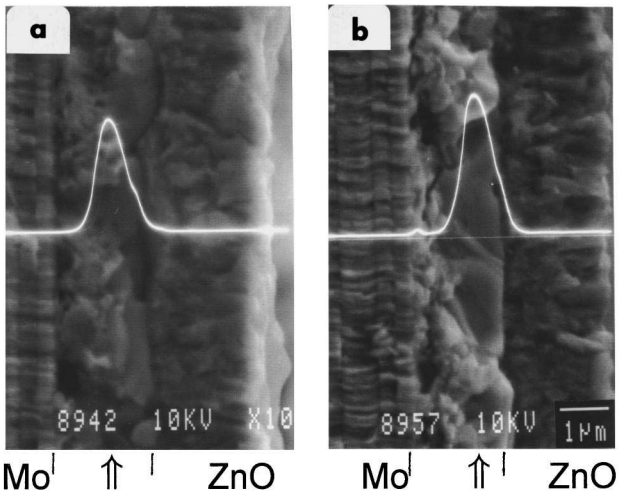

FIG. 4. Charge collection efficiency profiles (EBIC line scans) superimposed on scanning electron images of cross sections of samples (a) 1789-425 and (b) 1789-575. EBIC peak position is indicated with an arrow.

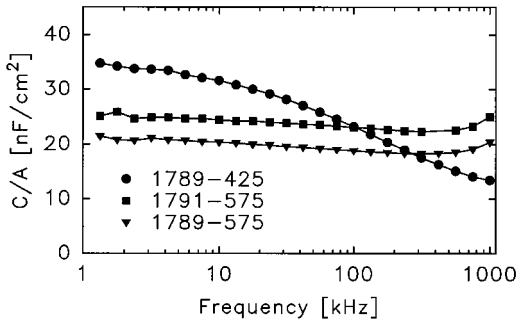

FIG. 5. Capacitance vs frequency data for the cells of Fig. 2.

575 °C. The peak position of the EBIC signal for sample 1789-425 indicates the electrical junction is significantly within the CIGS layer. The EBIC peak of sample 1789-575 is somewhat closer to the CIGS/CdS metallurgical junction.

Capacitance values of the three devices were measured as a function of frequency. The resulting $C(f)$ data taken under zero bias conditions in the dark are shown in Fig. 5. Capacitance–voltage ($C-V$) data obtained under near-steady-state conditions with 100 s wait at each bias point is given in Fig. 6(a) in the form of $(A/C)^2$ vs voltage curves.

The dispersion in the capacitance observed in Fig. 5 was the greatest for sample 1789-425, indicating the presence of a large density of extraneous states in the absorber. For this reason, the measurement frequency of $C-V$ data was increased from 60 to 500 kHz for this sample to minimize the apparent capacitance due to these extraneous states at lower frequencies. The zero bias capacitance value was the smallest for sample 1789-425, indicating the widest depletion width, despite the fact that the built-in potential was expected to be the smallest for this low-voltage device. The spatial variation of the hole density calculated from the slope of the Fig. 6(a) curves[12] is shown in Fig. 6(b) for the three cells. The distance from the metallurgical junction is determined directly from the measured capacitance. According to Fig. 6(b), the hole density in all films increases from less than 3×10^{15} cm^{-3} near the highly compensated surface region to about 3×10^{16} cm^{-3} at about 0.6–0.75 μm from the junction. Such a diode structure is intermediate between p-n and p-i-n. The width of the low-density region has a magnitude comparable to the depth of the EBIC peak, and it appears to decrease from sample 1789-425 to 1789-575. This observation suggests the existence of a highly compensated thick surface layer in sample 1789-425 and a decrease in the thickness of this compensated layer as the active Ga content in the absorber layer was increased by the high-temperature annealing step.

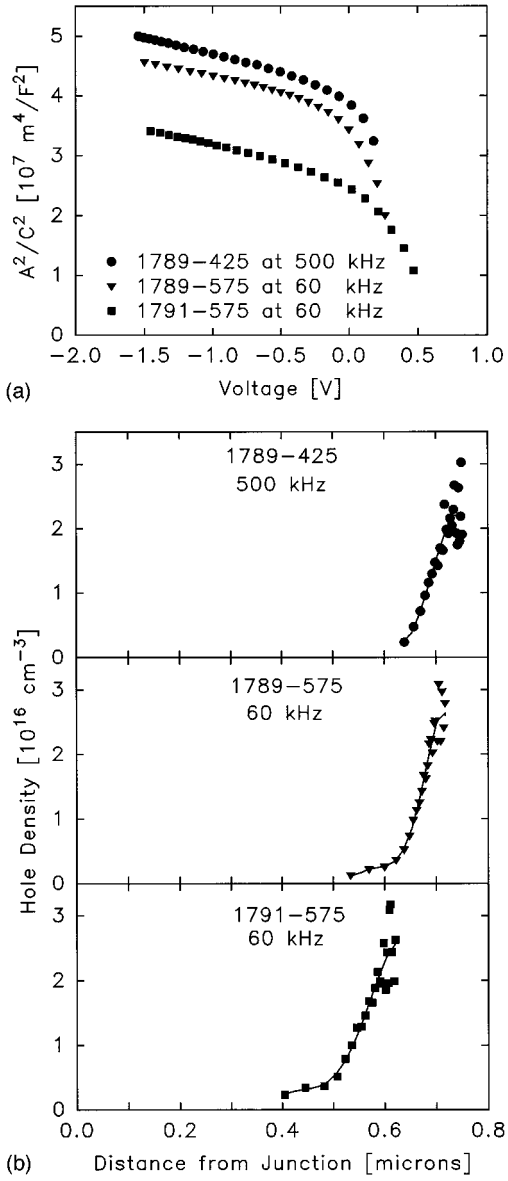

FIG. 6. (a) $(A/C)^2$ vs V, and (b) hole density distribution for the devices of Fig. 2.

B. Absorber layer characterization

Figure 7 shows the Auger depth profiles and the calculated Ga/(Ga+In) ratios of the CIGS films identified in Table I. As seen from these data, the compositions of samples 1789-425 and 1791-425, which were not subjected to the high-temperature annealing step after selenization, were highly graded suggesting segregation of In and Ga-rich phases. These films contained only small amounts of Ga near their surface, despite the fact that Ga was originally deposited on the surface of the precursor layers as described before. After the high-temperature annealing step, Ga concentration near the surface increased. However, the resulting absorbers were still graded in terms of their Ga distribution.

According to Fig. 7(a), the Ga/(Ga+In) ratio for sample 1789-425 increases from about 0.1 at a region about 0.1 μm inside the film surface to 0.98 at a depth of 1.4 μm. The expected E_g value of the surface region with 10% Ga is 1.07 eV, which is in good agreement with the data of Table II. The Ga/(Ga+In) ratios near the surface regions of samples 1789-575 and 1791-575 are 0.31 and 0.53, respectively. These values are also in reasonably good agreement with the device measurement results that predicted the presence of CIGS

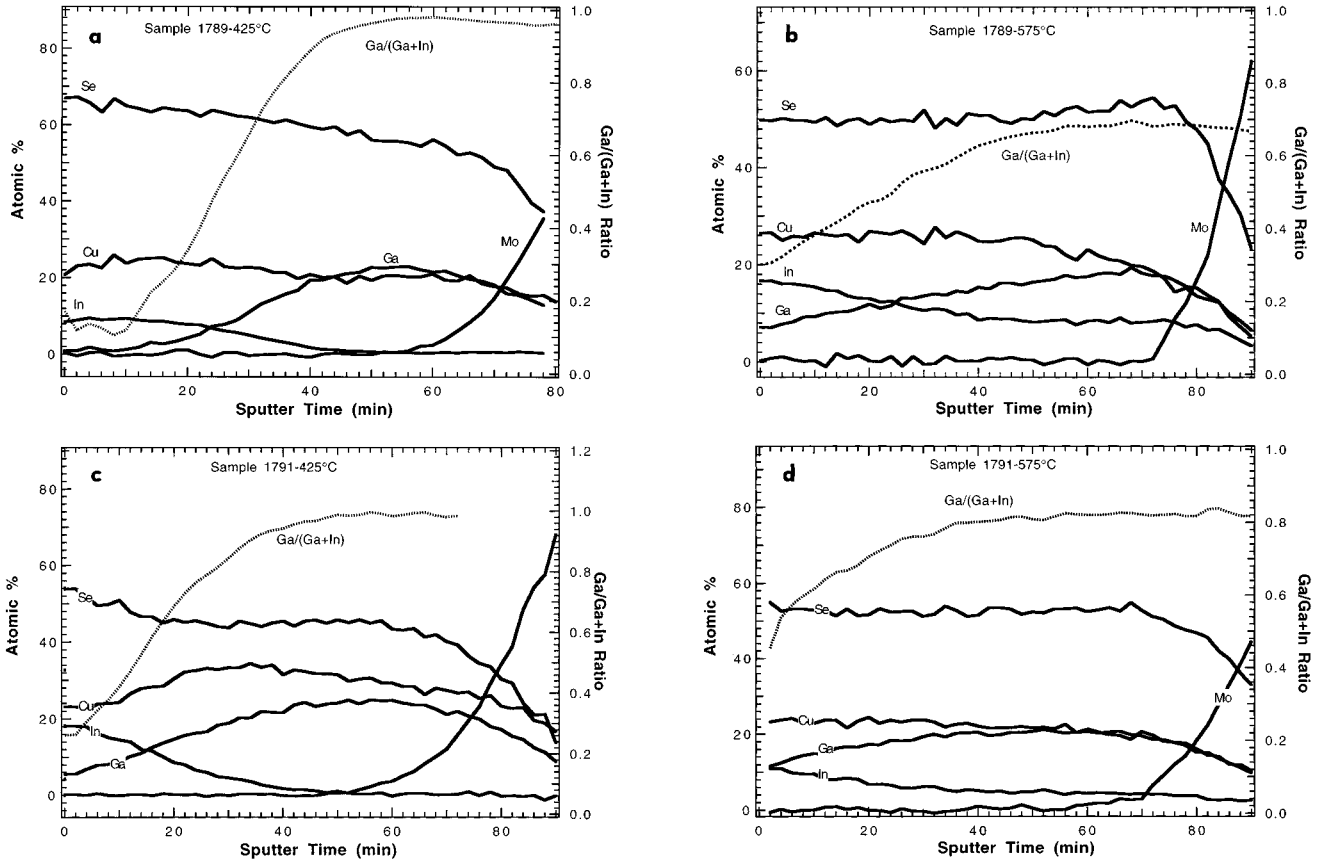

FIG. 7. Auger depth profiles of samples (a) 1789-425, (b) 1789-575, (c) 1791-425, and (d) 1791-575. The sputtering rate was 4–5 Å/s.

phases with 28% and 50% Ga, respectively, in these two absorber layers.

Although the Ga/(Ga+In) ratios deduced from the calibrated Auger data of Fig. 7 agreed well with the results obtained from QE and V_{oc} measurements, the Cu/(In+Ga) stoichiometric ratios of Fig. 7 were unrealistically high for samples 1789-425 and 1791-425. These ratios were in the range of 1.2–2.2, especially near the surface regions of the two films, despite the fact that the stoichiometric ratios of all the films studied were fixed at 0.9 at the precursor stage before the selenization step. Also noticeable in the Auger data of Figs. 7(a) and 7(c) were the excessively high Se concentrations, again especially near the surface regions of the two films. Both of these abnormalities disappeared once the films were annealed at 575 °C. For the samples of Figs. 7(b) and 7(d), the calculated Cu/(In+Ga) ratios approached 0.9 and Se concentration decreased to the 50%–53% range. We believe that the discrepancies observed between the Auger data of the two sets of films were due to the presence of binary phases in samples 1789-425 and 1791-425. The poor performance of the solar cell fabricated on sample 1789-425, its large capacitance dispersion, and the lack of photovoltaic activity for sample 1791-425, all support this argument. It is known that CGS formation requires higher temperatures than CIS formation.[6] Therefore, the selenization temperature of 425 °C used in this study, although quite adequate for the growth of high-quality CIS layers,[9,10] was not sufficient to form a CIS/CGS graded compound film, especially in the sample with high Ga content. Therefore, films containing the CIS phase as well as the CGS ternary and Ga–Se and Cu–Se binaries were formed as a result of the 425 °C selenization process. It should be noted that the Auger data of Fig. 7 were calibrated using sensitivity factors of elements obtained from electron microprobe analysis of quaternary compound CIGS standards. The presence of binary phases in the analyzed layers are expected to affect the atomic concentration values plotted in the Auger profiles, because the sensitivity factors of elements in the binaries will be different than those used for the calibration of the reported experiment.

X-ray diffraction (XRD) is another characterization tool that can give valuable information about the phase content of the absorber layers. Figure 8 shows the diffraction patterns obtained from two of the samples listed in Table I. Only the 2Θ values in the 44°–47° range have been scanned in this experiment to be able to resolve the (220) and (204) peaks of the tetragonal lattice. The expected positions of these peaks for CIS and CGS compounds were calculated using the data of Albin *et al.*,[1] and they are shown in Fig. 8. In sample 1789-425, the (220,204) peak belonging to tetragonal CIS is clearly resolved. The peak is shifted only slightly to higher angles suggesting inclusion of a small amount of Ga into the chalcopyrite absorber in agreement with the Auger and device measurements discussed before. Another observation

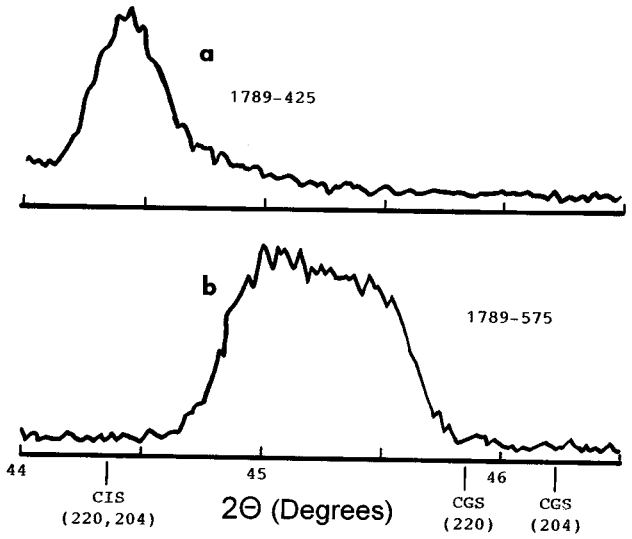

FIG. 8. XRD data taken from samples 1789-425 and 1789-575. The expected positions of the (220) and (204) peaks for CIS and CGS are indicated.

from Fig. 8(a) is the total absence of the (220) and (204) doublet peaks belonging to tetragonal CGS. The low temperature employed for selenization of this sample was not expected to form tetragonal CGS. There is a possibility, however, that the sphalerite phase of this compound was present in this film. X-ray data from sample 1789-575 did not display the merged CIS peaks of (220 and 204) at $2\Theta = 44.35°$. Instead, there is a broad peak shifted to higher angles indicating the formation of a CIGS phase. The shape of the peak suggests that the film is not uniform and that there is a compositional gradient through the absorber confirming the Auger results.

IV. CONCLUSIONS

Selenization of In/Cu/Ga precursors in a H_2Se atmosphere at a temperature of 425 °C yielded highly graded absorber layers, with CIS near the surface and Ga-rich compositions near the Mo/absorber interface. A high-temperature annealing step in a Se-free atmosphere promoted Ga diffusion and CIGS quaternary compound formation. Even Cu–In–Ga–Se layers containing ternary and binary compounds of CIS, Cu–Se, and Ga–Se which were not originally photoactive could be converted into device-quality CIGS films as a result of this annealing step. Solar cells with efficiencies near 12% were fabricated on these films. Longer heat treatment times and/or higher temperatures may be needed to obtain totally uniform CIGS absorbers by this technique.

ACKNOWLEDGMENTS

The authors gratefully acknowledge the in-depth discussion of the CIGS formation process with Dr. Robert Birkmire of IEC and thank Jennifer Granata of CSU for assistance in device measurements. This project has been funded by NREL Subcontract No. YI-2-12069-1.

[1]D. S. Albin, J. R. Tuttle, G. D. Mooney, J. J. Carapella, A. Duda, A. Mason, and R. Noufi, *Proceedings of the 21st IEEE PV Specialists Conference* (IEEE, New York, 1990), p. 562.
[2]M. A. Contreras, J. Tuttle, A. Gabor, A. Tennant, K. Ramanathan, S. Asher, A. Franz, J. Keane, L. Wang, J. Scofield, and R. Noufi, *Proceedings of the IEEE First World Conference on PV Energy Conversion, Hawaii* (IEEE, New Jersey, 1994), p. 68.
[3]W. H. Bloss, F. Pfisterer, M. Schubert, and T. Walter, Prog. Photovolt. **3**, 3 (1995).
[4]K. Kushiya, A. Shimizu, K. Saito, A. Yamada, and M. Konagai, in Ref. 2, p. 87.
[5]D. S. Albin, J. R. Tuttle, M. Contreras, A. M. Gabor, A. Mason, R. Noufi, and P. Singh, Sol. Energy Mater. Sol. Cells (in press).
[6]M. Marudachalam, R. Birkmire, J. M. Schultz, and T. Yokimcus, in Ref. 2, p. 234.
[7]B. M. Başol, V. K. Kapur, C. Leidholm, A. Halani, and A. Minnick, 13th NREL PV Program Review Meeting, Lakewood, Colorado, 16–19 May 1995 [AIP Conf. Proc. 353 (AIP, New York, 1996), p. 26].
[8]H. J. Von Bardeleben, Sol. Cells **16**, 381 (1986).
[9]B. M. Başol, V. K. Kapur, A. Halani, and C. Leidholm, Sol. Energy Mater. Sol. Cells **29**, 163 (1993).
[10]B. M. Başol, V. K. Kapur, and R. J. Matson, *Proceedings of the 22nd IEEE PV Specialists Conference* (IEEE, New York, 1991), p. 1179.
[11]R. J. Matson, Scan. Microsc. **2**, 121 (1988).
[12]S. M. Sze, *Physics of Semiconductor Devices*, 2nd ed. (Wiley, New York, 1981), p. 81.